Characterization of the attractor governing the neon bulb RC relaxation oscillator

M. L. Petrani,[1] Ch. Karakotsou,[2] I. M. Kyprianidis,[1] and A. N. Anagnostopoulos[2]
[1] *3rd Laboratory of Physics, Physics Department, University of Thessaloniki, Thessaloniki 54006, Greece*
[2] *1st Laboratory of Physics, Physics Department, University of Thessaloniki, Thessaloniki 54006, Greece*
(Received 24 May 1993; revised manuscript received 19 November 1993)

The sinusoidally driven neon bulb RC relaxation oscillator has been studied experimentally and its chaotic behavior has been verified. For certain values of the control parameters C (capacitance) and f_s (driving frequency) the observed response signal is nonperiodic. Calculation of the generalized dimensions shows that the system follows the quasiperiodicity route to chaos.

PACS number(s): 05.45.+b, 84.20.+m, 84.30.Ng, 85.10.Rg

INTRODUCTION

A driven negative-resistance oscillator circuit is a dissipative dynamical system of a type which very often exhibits chaotic behavior [1–3]. Its chaotic behavior can be described by deterministic nonlinear differential equations [4].

Experimental work performed on electric and electronic circuits has focused on the transition to chaos. Period doubling, intermittency, and formation of strange attractors are the well studied routes to chaos [5–7]. Frequency locking and period adding are the most investigated effects in different nonlinear circuits [8,9].

We use the Grassberger-Proccacia method [10] to measure the dimensionality of the attractor produced by a simple experimental circuit with a nonlinear I-V characteristic. The circuit examined is the classical neon bulb RC relaxation oscillator, Fig. 1, in which van der Pol and van der Mark first observed nonlinearity in 1927 [11]. Recently, Kennedy and Chua reexamined the same circuit and found an alternating sequence of chaotic and periodic regimes, one of the first examples of the period-adding route to chaos [12].

EXPERIMENTAL

A. Experimental setup

The circuit we consider, Fig. 1, is the sinusoidally driven neon bulb relaxation oscillator, described and studied in Refs. [11–13]. A high-voltage dc power supply E is attached to the shunt connection of a neon bulb and to a precision variable capacitor C forming the basic relaxation oscillator. A digital frequency generator and a small precision resistor R_s are inserted in series with the neon bulb. The voltage supply E, with 100 V terminal voltage and a comparatively large output resistance R ($R = 1.1$ MΩ) was checked for stability to avoid undesired ripple factor. The frequency generator acted as a sinusoidal voltage source $u_s = E_0 \cos\omega t$, while the small resistor $R_s (R_s = 60\ \Omega)$ sensed the current flowing through the neon bulb. The static resistance of the neon bulb in the Ohmic region of its I-V characteristic was 10^7 Ω. All the cables used were coaxial and the experimental setup was electromagnetically shielded to avoid external influences, like radio frequency interference (RFI) pickup.

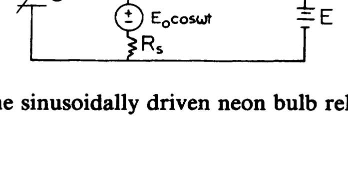

FIG. 1. The sinusoidally driven neon bulb relaxation oscillator.

B. Measurements

The voltage wave forms both across the capacitor C and across the resistor were measured. As explained in

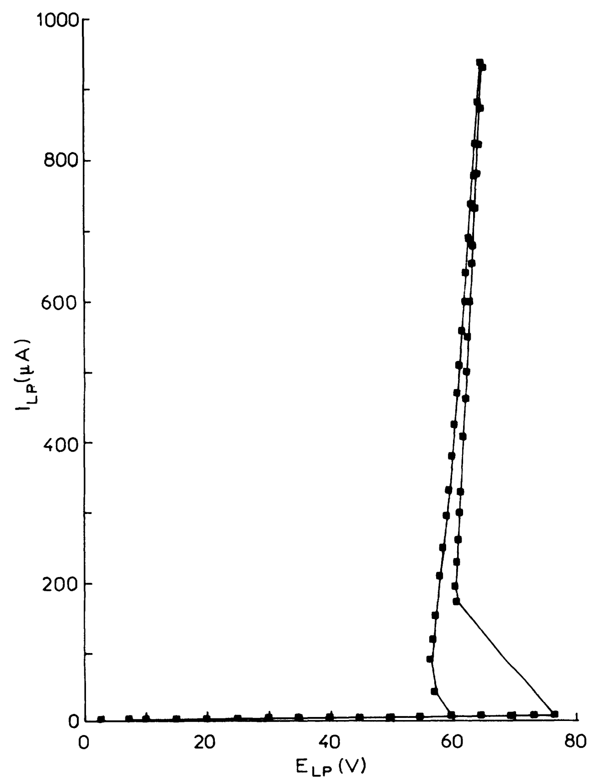

FIG. 2. The static I-V characteristic of the neon bulb.

1063-651X/94/49(6)/5863(4)/$06.00

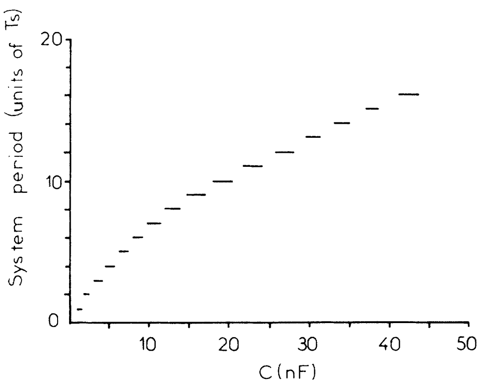

FIG. 3. Pulse pattern repetition rate vs C, showing the coarse staircase structure.

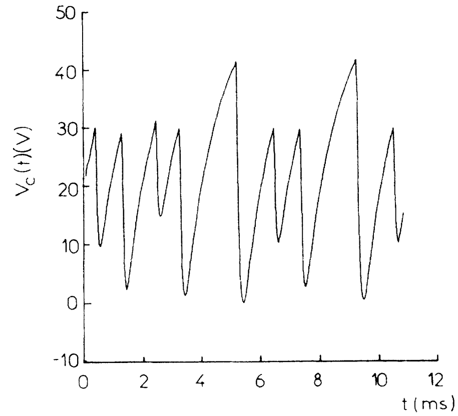

FIG. 4. The response signal obtained for $C=1.7$ nF, $R=1.1$ MΩ, and $f_s=1$ kHz.

Ref. [13] the measurement of the voltage drop across the capacitor C seemed to be more advantageous, but the wave forms monitored across the resistor R_s showed more pronounced chaotic behavior.

The measured voltages were monitored on a digital oscilloscope (Hameg HM-408). An IBM PC-AT was used as an IEEE-488 controller as well as to display the results obtained. With the signal source zeroed, the natural frequency of the undriven oscillator was set to 1 kHz by tuning capacitance C to $C_0=1$ nF. Then a sinusoidal signal of amplitude 8 V and frequency 1 kHz was applied. The static I-V characteristic is shown in Fig. 2.

As the capacitance C was increased, a coarse staircase structure, similar to that of Kennedy and Chua [12] was obtained (Fig. 3).

Next, the capacitance was kept constant and the frequency f_s of the drive signal was increased. For $C=30$ nF, and $R=100$ kΩ, subharmonics were observed with a period up to 31 times the period of the drive signal. Kennedy and Chua observed subharmonics only up to 20 times the period of the drive signal [12]. At high frequencies there are no more subharmonics. Instead the two signals synchronize 1:1.

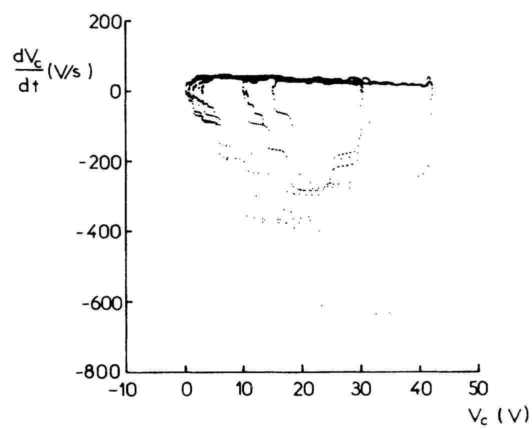

FIG. 5. The phase portrait corresponding to the signal of Fig. 4. The chaotic three-banded structure of the attractor, formed by the trajectories, is obvious in this plot.

DIMENSIONS AND HOMOGENEITY OF THE ATTRACTOR

For $C=1.7$ nF and $f_s=1$ kHz we obtained the signal shown in Fig. 4. The signal seems to be nonperiodic. The corresponding phase portrait of this signal is shown in Fig. 5. In Fig. 6 the power spectrum of this signal is presented. The presence of a chaotic three-banded attractor, formed by the trajectories in Fig. 5, and the existence of corresponding pronounced peaks, indicated by arrows at the frequencies f_2, f_4, and f_6 in Fig. 6, clearly indicate the nonperiodic nature of the signal of Fig. 4. The frequencies f_2, f_4, and f_6 have the following values:

$$f_2=0.46 \text{ kHz}, \quad f_4=1.02 \text{ kHz}, \text{ and } f_6=1.49 \text{ kHz} .$$

The satellite frequencies of f_2, f_4, and f_6 contribute to the dispersion and the subsequent formation of the three-banded phase portrait in Fig. 5.

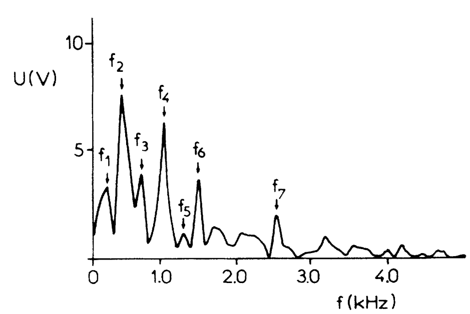

FIG. 6. The power spectrum corresponding to the signal of Fig. 4. Note the coexistence of pronounced peaks, f_2, f_4, and f_6, corresponding to the three-banded structure of the attractor of Fig. 5.

To obtain a quantitative measure of the chaos present in the signal of Fig. 4 we followed the well-known method of calculating the generalized dimensions D_q of our system and the corresponding $f(\alpha)$ spectrum. This method [14] has already been applied in similar cases [15–17]. The phase space is divided into hypercells with a linear dimension l. For increasing values of l, we count all points with mutual distances less than l, and we calculate the correlation integral $C^q(l)$ via the relation [18]

$$C^q(l)=\sum_i p_i^q=\frac{1}{N}\sum_{ij}^{N}\left[\frac{1}{N}\sum_{ij}^{m}\Theta(l-|x_i-x_j|)\right]^{q-1} . \quad (1)$$

The generalized dimensions D_q are connected with $C^q(l)$ via the relation [14]

$$D_q=-\lim_{l\to 0}\frac{1}{q-1}\frac{\ln C^q(l)}{\ln l} . \quad (2)$$

The D_q's measure correlations between different points of the attractor and are, therefore, useful in characterizing its inhomogeneous static structure. For $q=0$, D_0 is the ordinary fractal dimension of the attractor. For q large and positive D_q's give information about the dense regions of the attractor. For q large and negative, D_q's give information about the sparse regions of the attractor.

Drawing $C^q(l)$ vs l in a double-logarithmic plot with q as a parameter we can obtain the values

$$\tau_q=\ln C^q(l)/\ln l , \quad (3)$$

from the slope of the linear parts of the corresponding curves for low l values. To select the correct linear parts of these curves we have taken into account the remarks included in Refs. [16 and 19].

The calculation of the slope $\ln C^q(l)/\ln l$ is a kind of generating function, which can be used to determine the function $f(\alpha)$ via the pair of equations [14,20]

$$\alpha(q)=\frac{\partial}{\partial q}[(q-1)D_q] , \quad (4a)$$

$$f(\alpha)=q\alpha-[q-1]D_q . \quad (4b)$$

Using Eqs. (4) we obtain the experimental $f(\alpha)$ spectrum presented by curve a in Fig. 7, from which it follows that $D_0=f_{\max}(\alpha)=1.03, D_{+\infty}=\alpha_{\max}=1.46$, and $D_{-\infty}=\alpha_{\min}=0.87$. The theoretical $f(\alpha)$ curve, for the ideal quasiperiodic transition to chaos, is presented by curve b in the same figure.

The maximum value of the experimental $f(\alpha), D_0$, is only slightly above unity and corresponds to a value of α, α_0, also very close to unity ($\alpha_0=1.1$). According to Su, Rollins, and Hunt [16], this means that the $f(\alpha)$ spectrum, shown in Fig. 7, corresponds exactly to the transition of the system from the quasiperiodic to the chaotic state. For subcritical orbits, the maximum value of the $f(\alpha)$ spectrum should be just below unity, while for supercritical orbits becomes higher than unity. Since our system is in a critical state, the deviation of the experimental $f(\alpha)$ curve from the ideal one has to be attributed to the existence of the third frequency observed in the power spectrum (Fig. 6).

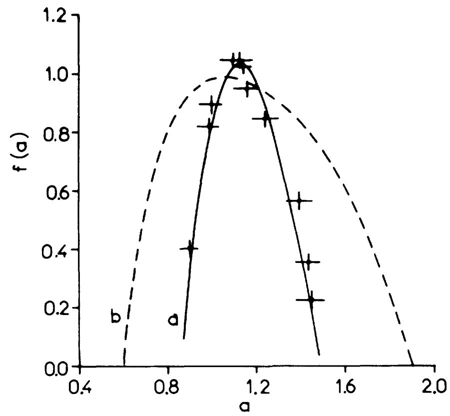

FIG. 7. $f(\alpha)$ curves for (a) the experimental signal of Fig. 4 and (b) the ideal quasiperiodic transition to chaos, at the same frequency ratio 23/51.

The form of curve a in Fig. 7, and the obtained values of D_0, $D_{+\infty}$, and $D_{-\infty}$, indicate that our system shows similar behavior to quasiperiodic systems already reported in the literature [21–24].

DISCUSSION

D_0 is not much higher than unity, as for a quasiperiodic attractor. This conclusion is corroborated by the presence of the three distinct frequencies in the power spectrum of Fig. 6. Furthermore, the phase portrait of Fig. 5 obviously consists only of three quasiperiodic trajectories; each a little dispersed. One might think that the voltage wave form shown in Fig. 4 consists only of fully periodic signals superimposed on each other, but the simultaneous appearance of three incommensurate frequencies is related to the quasiperiodicity route to chaos [21,22]. Chaos becomes noticeable in the dispersion of the quasiperiodic trajectories on the phase plane (Fig. 5), in the broadband background of the power spectrum (Fig. 6), in the lack of fully developed periodicity in the signal of Fig. 4, and in the small deviation of D_0 from unity.

[1] J. Guckenheimer and P. Holmes, *Nonlinear Oscillations, Dynamical Systems and Bifurcations of Vector Fields* (Springer-Verlag, NY, 1983).
[2] F. C. Moon, *Chaotic Vibrations* (Wiley, NY, 1987).
[3] M. J. Hasler, Proc. IEEE **75**, 1009 (1987).
[4] E. A. Jackson, *Perspectives of Nonlinear Dynamics* (Cambridge University Press, Cambridge, 1989).
[5] P. S. Linsay, Phys. Rev. Lett. **47**, 1349 (1981).
[6] K. Fukushima and T. Yakiada, J. Phys. Soc. Jpn. **57**, 4055 (1988).
[7] T. Matsumoto, L. O. Chua, and M. Komuro, IEEE Trans. Circuits Syst. **CAS-32**, 797 (1985).
[8] J. A. Glazier and A. Libchaber, IEEE Trans. Circuits Syst. **CAS-35**, 790 (1988).

[9] L. Q. Pei, F. Guo, S. X. Wu, and L. O. Chua, IEEE Trans. Circuits Syst. **CAS-33**, 438 (1986).

[10] P. Grassberger and J. Procaccia, Phys. Rev. Lett. **50**, 346 (1983).

[11] B. van der Pol and J. van der Mark, Nature **120**, 363 (1927).

[12] M. P. Kennedy and L. O. Chua, IEEE Trans Circuits Syst. **CAS-33**, 974 (1986).

[13] M. P. Kennedy, K. R. Krieg, and L. O. Chua, IEEE Trans. Circuits Syst. **CAS-36**, 1133 (1989).

[14] For a good review see, H. G. Schuster, *Deterministic Chaos* (VCH, Weinheim, 1989), Chap. 5.

[15] Z. Su, R. W. Rollins, and E. R. Hunt, Phys. Rev. A **36**, 3573 (1987).

[16] Z. Su, R. W. Rollins, and E. R. Hunt, Phys. Rev. A **40**, 2689 (1989).

[17] J. A. Glazier, G. Gunaratne, and A. Libchaber, Phys. Rev. A **37**, 525 (1988).

[18] P. Grassberger and J. Procaccia, Physica D **9D**, 189 (1983).

[19] E. Gwinn and R. M. Westervelt, Phys. Rev. Lett. **59**, 157 (1987).

[20] H. Atmanspacher, H. Scheingraber, and W. Voges, Phys. Rev. A **37**, 1314 (1988).

[21] S. Martin, H. Leber, and W. Martiensen, Phys. Rev. Lett. **53**, 303 (1984).

[22] A. Libchaber, S. Fauve, and C. Laroche, Physica D **7D**, 73 (1983).

[23] Th. Schneider, H. Heng, and W. Martiensen, Europhys. Lett. **22**, 499 (1993).

[24] D. J. Biswas and R. G. Harrison, Phys. Rev. A **32**, 3835 (1985).